JOURNAL OF CATALYSIS 138, 536–546 (1992)

Role of Silver Promoter in Carbon Monoxide Hydrogenation and Ethylene Hydroformylation over Rh/SiO_2 Catalysts

STEVEN S. C. CHUANG[1] AND SHYH-ING PIEN

*Department of Chemical Engineering, The University of Akron, Akron, Ohio 44325

Received April 6, 1992; revised July 11, 1992

The effect of silver promotion on CO hydrogenation and ethylene hydroformylation over Rh/SiO_2 has been studied. Catalyst characterization before reaction reveals that Ag and Rh form separate crystallites; part of the Ag is atomically spread on the surface of Rh crystallite and blocks the Rh ensembles required for the bridge CO. Although both reactions restructure the catalyst surface and increase the ratio of bridge to linear CO sites on $Ag–Rh/SiO_2$ catalysts, the ratio of the bridge to the linear CO sites remains lower on $Ag–Rh/SiO_2$ than on Rh/SiO_2 under reaction conditions. Ag is found to increase the selectivity and the rate of formation for acetaldehyde (C_2 oxygenate) during CO hydrogenation and for propionaldehyde (C_3 oxygenate) during ethylene hydroformylation on Rh/SiO_2. The increased activity and selectivity for C_2 and C_3 oxygenates is attributed to a high ratio of the linear CO to bridge CO sites and a possible presence of isolated Rh^+ sites under reaction conditions. The results are consistent with a previous report that the single Rh atom site that chemisorbs linear CO is active for CO insertion.

INTRODUCTION

Supported Rh catalysts have been a subject of extensive studies because of its unique activity for C_2 oxygenate synthesis (*1–30*). Several mechanistic studies have suggested that the formation of C_2 oxygenates occurs via a number of elementary steps: dissociation of CO to produce surface carbon, hydrogenation of surface carbon to form adsorbed methyl species, insertion of CO into adsorbed methyl species to form adsorbed acyl species, and hydrogenation of acyl species to form either acetaldehyde or ethanol. The selectivity of Rh catalysts to C_2 oxygenates lies in their CO insertion and dissociation activities (*5, 7–9, 11–15, 18*).

The CO insertion step leading to the formation of C_2 oxygenates on supported Rh catalysts was proposed on the basis of the mechanism of homogeneous hydroformylation (*4–9, 18, 24, 25, 30*). The insertion of CO into a metal–alkyl bond has been widely studied and well established in the field of organometallic chemistry; CO insertion has been shown to be a key step in homogeneous olefin hydroformylation and alcohol carbonylation (*30–39*). The apparent similarity between CO insertion on metal carbonyls and on supported metals has led to the use of ethylene hydroformylation as a probe reaction to determine the CO insertion activity of supported Rh catalysts (*7, 14, 15, 17, 18, 24, 25, 30*). Although propionaldehyde is a minor product in ethylene hydroformylation on supported metals, the selectivity to propionaldehyde usually correlates with the selectivity to C_2 oxygenate in CO hydrogenation. This observation of hydroformylation activity of supported Rh catalysts suggests that the CO insertion selectivity of supported Rh catalysts may be further improved to compete with homogeneous hydroformylation catalysts (*40*).

A large number of studies have shown that the CO hydrogenation selectivity of Rh catalysts greatly depends on the compositions of supports and promoters (*1–30*). Rh on pure SiO_2 and Al_2O_3 supports produces mainly hydrocarbons, while Rh on TiO_2 and La_2O_3 produces primarily acetaldehyde and

[1] To whom correspondence should be addressed.

0021-9517/92 $5.00

ethanol at 0.1–3 MPa and 433–573 K (*2, 3, 5, 9, 27*). Methanol formation on Rh is enhanced by the use of ZnO, CaO, and MgO as supports. Promoters, including Mn, Zr, Ti, V, and La oxides, have been demonstrated to enhance C_{2+} oxygenate selectivity over Rh catalysts. Alkali promoters selectively inhibit hydrogenation, leading to the enhancement of C_2 oxygenate selectivity (*17*).

Modification of catalyst activity and selectivity by various promoters (additives) has been summarized as follows (*11, 14, 17, 21, 22, 28*): (i) the blockage of surface sites by the presence of additives, (ii) the interaction of additives with reactant molecules and reaction intermediates, and (iii) the modification of catalyst states by the electronic effect of additives. The physical blockage of active sites by additives, such as Zn and Fe, has a great effect on CO dissociation, which requires large ensembles of surface atoms (*11, 12, 16*). Mn, Ti, and Zr promoters tend to interact with the oxygen atom of CO; such an interaction could enhance either CO insertion or CO dissociation (*11*). The electronic effects of additives, such as alkali promoters, are known to increase CO adsorption energy and the CO dissociation activity and to suppress hydrogenation (*14, 17*).

Ag, whose electronegativity is similar to that of Rh metal, is an inactive element for a number of reactions, including CO hydrogenation, olefin hydrogenation, and alkane hydrogenolysis (*41–47*). Due to the inertness and electroneutrality of Ag, Ag–Rh catalysts provide an excellent model system for studying the geometric effect of additives on CO hydrogenation and ethylene hydroformylation. Methanation studies on Ag–Rh(111) single crystal found that Ag blocked Rh sites on a one-to-one basis (*41, 42*). Our previous CO hydrogenation study has shown that Ag decreases the rate of hydrocarbon formation more than it does that for C_2 oxygenates, resulting in a marked increase in C_2 oxygenate selectivity (*44*). The difference in suppression of product formation by Ag suggests that C_2 oxygenate synthesis may be less structure sensitive than hydrocarbon synthesis.

The objective of this study was to investigate the effect of Ag on CO adsorption, CO hydrogenation, and ethylene hydroformylation on Rh/SiO_2 catalysts. The surface states and structures of $Ag–Rh/SiO_2$ catalysts were studied by X-ray photoelectron spectroscopy, infrared spectroscopy of NO and CO adsorption, and ethane hydrogenolysis. The structure of chemisorbed CO during reaction was determined by *in situ* infrared spectroscopy.

EXPERIMENTAL

The SiO_2-supported Ag–Rh catalysts were prepared by incipient wetness coimpregnation of SiO_2 (Strem Chemicals) with an aqueous solution of Rh and Ag nitrates (Alfa Chemicals). The Rh/SiO_2 was prepared by the same method using Rh nitrate solution. Each gram of silica was impregnated with 0.9 cm^3 of solution. The Rh loading is 3 wt% for Rh/SiO_2 and all $Ag–Rh/SiO_2$ catalysts. The $Ag–Rh/SiO_2$ catalysts with molar ratios of Ag to Rh of 0.25, 0.5, and 1 are denoted as $Ag(0.25)Rh/SiO_2$, $Ag(0.5)Rh/SiO_2$, and $Ag(1)Rh/SiO_2$, respectively. After impregnation, the samples were dried overnight in air at 313 K, then reduced in flowing hydrogen at 673 K for 16 hr.

Average Ag and Rh crystallite sizes were determined by a Phillips APD3700 X-ray diffractometer using a line-broadening technique. Hydrogen chemisorption was evaluated from the area under a hydrogen temperature-programmed desorption (TPD) curve. Adsorption of hydrogen was carried out by flowing hydrogen through the TPD reactor at 303 K. The X-ray photoelectron spectroscopy (XPS) of the catalysts was obtained by a Leybold LHS-10 system equipped with a high-pressure sample preparation facility which allows various pretreatments of the catalyst and transfer of the catalyst sample to the vacuum chamber without exposure to air. Binding energies

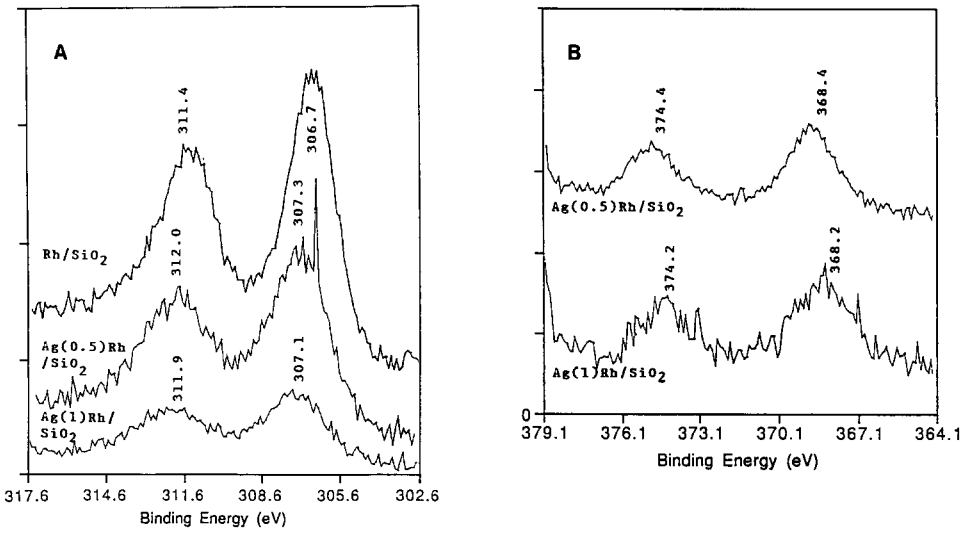

FIG. 1. (A) XPS spectra of Rh/SiO_2 and $Ag–Rh/SiO_2$: Rh $3d_{3/2}$ and Rh $3d_{5/2}$. (B) XPS spectra of $Ag(0.5)Rh/SiO_2$ and $Ag(1)Rh/SiO_2$: Ag $3d_{3/2}$ and Ag $3d_{5/2}$.

were referenced to the Si^{4+} $2p_{1/2}$ peak at 103.5 eV, which yielded the $1s$ binding energy of the adventitious carbon on the catalyst sample in the 284.9–285.1 eV range.

The catalyst sample (25 mg) was pressed into a self-supporting disk and placed in an IR cell for infrared study (*30*). Infrared spectra of adsorbed CO and NO at 301 K were recorded by a Nicolet 5SXC FTIR spectrometer at a resolution of 4 cm^{-1}. Gas-phase CO bands were eliminated by subtracting the absorbance of gas-phase CO with a SiO_2 disk in the cell from the spectra of adsorbed species on the Rh/SiO_2 and $Ag–Rh/SiO_2$ catalysts.

Ethane hydrogenolysis ($C_2H_6 : H_2 = 1 : 6$) was performed in a stainless-steel differential reactor at 493 K and 0.1 MPa. CO hydrogenation ($CO : H_2 = 1 : 1$) and ethylene hydroformylation ($C_2H_4 : CO : H_2 = 1 : 1 : 1$) were studied under steady-state flow conditions of 513 K and 1–2 MPa in an IR cell, which can be considered a differential reactor. The effluent of the IR cell was sampled every 30 min during reaction and analyzed by an on-line HP-5890A gas chromatograph (GC) with a Porapak PS column. Steady-state activity and product distribution were achieved after 90 min of reaction.

RESULTS

X-Ray Photoelectron Spectroscopy

Figures 1A and 1B show the XPS spectra of Rh/SiO_2 and $Ag–Rh/SiO_2$ taken after reduction at 513 K. The Rh/Si and Ag/Rh intensity ratios are presented in Table 1. The Rh $3d_{3/2}$ and $3d_{5/2}$ binding energies for the Rh/SiO_2 catalyst were observed at 311.4 and 306.7 eV, respectively. Oxidation of the Rh/SiO_2 catalyst resulted in an upward shift of 0.8–0.9 eV (*30*). The addition of Ag to Rh/SiO_2 caused an upward shift of the Rh $3d_{3/2}$ and $3d_{5/2}$ binding energies to 312 and 307 eV and an increase in the intensity ratio of Ag to Rh peaks. The binding energy for Rh on $Ag–Rh/SiO_2$ catalysts falls between those for the reduced Rh/SiO_2 and for the oxidized Rh/SiO_2. The results indicate that the oxidation state of Rh on the $Ag–Rh/SiO_2$ catalyst is between 0 and +1. The Ag $3d_{5/2}$ binding energy was observed at 368.2 eV for $Ag(0.5)Rh/SiO_2$ and at 368.4 eV for $Ag(1)Rh/SiO_2$ following hydrogen reduction at 513 K. These binding energies cor-

TABLE 1

Catalyst Characterization

Catalyst	XPS peak intensity ratio		IR intensity ratio of	Crystallite size (Å, XRD)		Hydrogen chemisorption (μmole/g)	Ethane hydrogenolysis at 493 K × 10^3 (sec^{-1})
	Rh/Si	Ag/Rh	bridge CO / linear CO	Rh	Ag		
Rh/SiO_2	0.3	—	1.23	87[a]	—	39.2	2.7
$Ag–Rh/SiO_2$ (0.5 : 1)	0.19	0.26	0.51	85	468	24.0	0.87
$Ag–Rh/SiO_2$ (1 : 1)	0.14	0.79	0.33	136	395	5.4	1.7

[a] Determined after reaction studies.

respond to the oxidation state of more than +1 for Ag.

CO Adsorption

Figure 2 shows the infrared spectra of CO adsorption on Rh/SiO_2 catalysts with different Ag loadings at 301 K and 0.1 MPa. CO adsorption on Ag/SiO_2 did not produce adsorbed CO species at 301 K, confirming that Ag is an inactive component for CO-related reactions. Two bands at 2060 and 1874 cm^{-1} observed for the Rh/SiO_2 catalyst are assigned to the linear and bridged CO on Rh

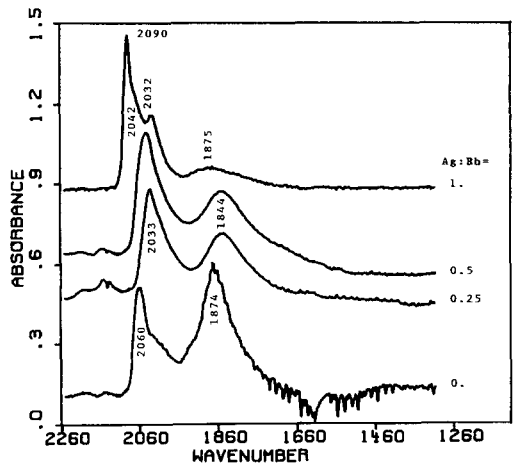

FIG. 2. Infrared spectra of adsorbed CO on Rh/SiO_2 and $Ag–Rh/SiO_2$ at 301 K.

crystallite, respectively (*30, 44, 48–55*). The presence of Ag on the $Ag(0.25)Rh/SiO_2$ and $Ag(0.5)Rh/SiO_2$ decreased the wavenumber of linear and bridge CO bands and the intensity ratio of the bridge CO to the linear CO band. The downward shift of the CO band indicates that Ag decreases the dipole–dipole coupling between neighboring adsorbed CO (*56*); the decreased intensity ratio of the bridge to linear CO suggests that the Ag additive blocks the bridge CO sites.

As the Ag/Rh ratio increased to 1, a new band at 2090 cm^{-1} was formed and the intensity of the bridge CO band was significantly reduced. The unusually high intensity ratio of the 2090 cm^{-1} band to the 2032 cm^{-1} band is very likely due to the asymmetric component of the gem-dicarbonyl band and a linear CO species on a Rh^+ site. Linear CO adsorbed on Rh^+ is known to give an IR band in the 2100–2090 cm^{-1} region (*30, 52*).

NO Adsorption

Figure 3 shows the infrared spectra of NO adsorption on Rh/SiO_2 catalysts with different Ag loading. The observed IR spectra of NO on Rh/SiO_2 agree well with previous studies (*57–59*). The doublet and the tip at 1875 cm^{-1} are due to P, R, and Q branches of the vibrational–rotational spectra of gaseous NO; the R branch of the NO spectra is overlapped with a band at 1851–1859 cm^{-1},

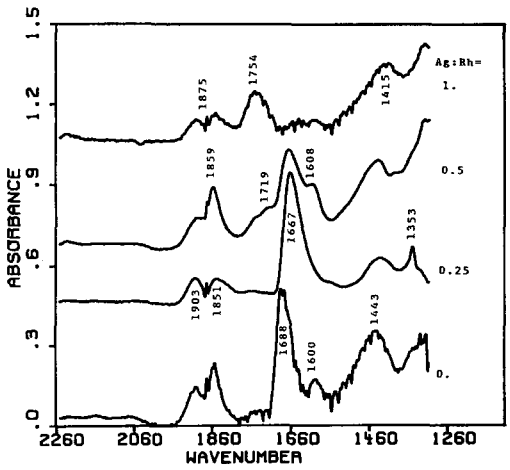

FIG. 3. Infrared spectra of NO adsorption on Rh/SiO_2 and $Ag–Rh/SiO_2$ at 301 K.

which has been assigned to the linear NO on Rh (the neutral nitrosyl species) (*57, 58*). The species and gaseous NO can be completely removed with flowing nitrogen at 301 K. The bands in the 1660–1760 cm^{-1} region can be assigned to a surface anionic NO (NO^-); the band in the 1443–1415 cm^{-1} region is characteristic of nitrato species NO_2^- and NO_3^- (*58*). The NO^- band is drastically affected by the presence of Ag. A band near 1719 cm^{-1} emerged as a shoulder of the NO^- band on the $Ag(0.5)Rh/SiO_2$ catalyst. The NO^- band shifted upward to 1754 cm^{-1} on the $Ag(1)Rh/SiO_2$ catalyst. The shift in the wavenumber of adsorbed NO suggests that Ag affects the electronic state of the Rh surface.

CO Hydrogenation

Figure 4 shows the infrared spectra for CO hydrogenation over Rh/SiO_2, $Ag(0.5)Rh/SiO_2$, and $Ag(1)Rh/SiO_2$ catalysts. Little variation of infrared spectra with time was observed at each reaction condition. The steady-state rates of product formation corresponding to the infrared spectra are presented in Table 2. Methane was the major product; acetaldehyde and C_2–C_3 hydrocarbons were minor products over the Rh/SiO_2 catalyst at 513 K and 1 MPa. Under the same condition, the infrared spectrum shows linear CO and bridged CO bands at 2035 and 1843 cm^{-1}, respec-

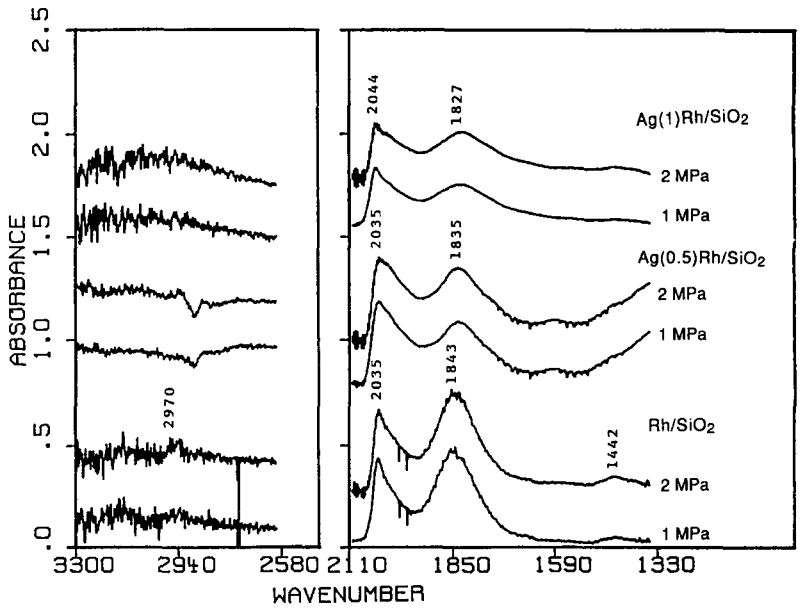

FIG. 4. Infrared spectra of adsorbed species during CO hydrogenation at 513 K.

TABLE 2

CO Hydrogenation at 513 K

Catalyst	Pressure (MPa)	CO conversion		Selectivity					Product ratio
		TOF × 10^3 (sec^{-1})	Rate mole/kg-hr	CH_4	C_2H_4	C_2H_6	C_{3+}HC (mole%)	CH_3CHO	$\frac{CH_3CHO}{CH_4}$
Rh/SiO_2	1	2.8	0.79	67.9	1.0	23.1	0.5	7.5	0.11
	2	3.6	1.03	63.2	10.2	18.5	0.7	7.4	0.12
Ag–Rh/SiO_2	1	0.9	0.15	91.6	2.0	—	—	6.4	0.07
(0.5 : 1)	2	1.6	0.28	71.6	17.0	0.4	—	11.0	0.15
Ag–Rh/SiO_2	1	10.2	0.40	59.6	16.3	1.8	8.4	13.9	0.23
(1 : 1)	2	13.2	0.51	47.6	16.6	0.9	6.5	28.4	0.60

Note. $CO : H_2 = 1 : 1$; selectivity = the rate of formation of a specific product/the rate of formation of all the products.

tively. An increase in reaction pressure to 2 MPa caused a slight variation in infrared spectra of adsorbed CO and rates of product formation.

The presence of Ag on Rh/SiO_2 led to a decrease in the selectivity for methane and C_2 hydrocarbon formation, but an increase in selectivity and rate of formation for acetaldehyde. It should be noted that the TOF in Table 2 was estimated using the number of Rh surface atoms determined by H_2 temperature-programmed desorption before reaction. The number of Rh surface atoms before reaction may not correspond to that during reaction. The extent of Ag effects was progressively increased from Ag(0.25)Rh/SiO_2 to Ag(1)Rh/SiO_2 (*44*). Infrared spectra corresponding to rate and selectivity data show that increasing the Ag/Rh ratio decreased the ratio of intensity of bridge to linear CO bands. However, the extent of decrease in the intensity ratio of bridge CO to linear CO bands is smaller for the catalysts under CO hydrogenation conditions than those under CO adsorption at 301 K. Increasing reaction pressure from 1 to 2 MPa increased the rate and selectivity for acetaldehyde formation on Ag(0.5)Rh/SiO_2 and Ag(1)Rh/SiO_2 catalysts. The effect of pressure on product selectivity is much more pronounced on Ag–Rh/SiO_2 than on Rh/SiO_2 catalysts. However, an increase in pressure did not lead to an appreciable change in the infrared spectra of adsorbed CO.

Ethylene Hydroformylation

Figure 5 shows the infrared spectra of the steady-state ethylene hydroformylation over Rh/SiO_2, Ag(0.5)Rh/SiO_2, and Ag(1)Rh/SiO_2 catalysts. The steady-state selectivity data corresponding to the infrared spectra are presented in Table 3. Ethane and propionaldehyde were the major products; methane, C_{3+} hydrocarbons, and acetaldehyde were the minor products over the Rh/SiO_2 catalyst at 513 K and 1 MPa. Under identical conditions, the infrared spectra show a linear CO band in the 2015–2025 cm^{-1} region. The bridged CO band is overlapped by gaseous ethylene at 1919, 1888, and 1850 cm^{-1}. The band near 1730 cm^{-1} is assigned to propionaldehyde. The bands in the 3140–2700 cm^{-1} region are due to C–H stretching. The bands at 3138 and 3067 cm^{-1} are exhibited by gaseous ethylene; the band at 2899 cm^{-1} is due to gaseous ethane; and the band at 2720 cm^{-1} is characteristic of the C–H stretching of propionaldehyde (*60*).

The presence of Ag on Rh/SiO_2 suppressed the selectivity for methane and ethane formation but enhanced the selectivity and rate of formation for propionaldehyde. The addition of Ag also significantly reduced

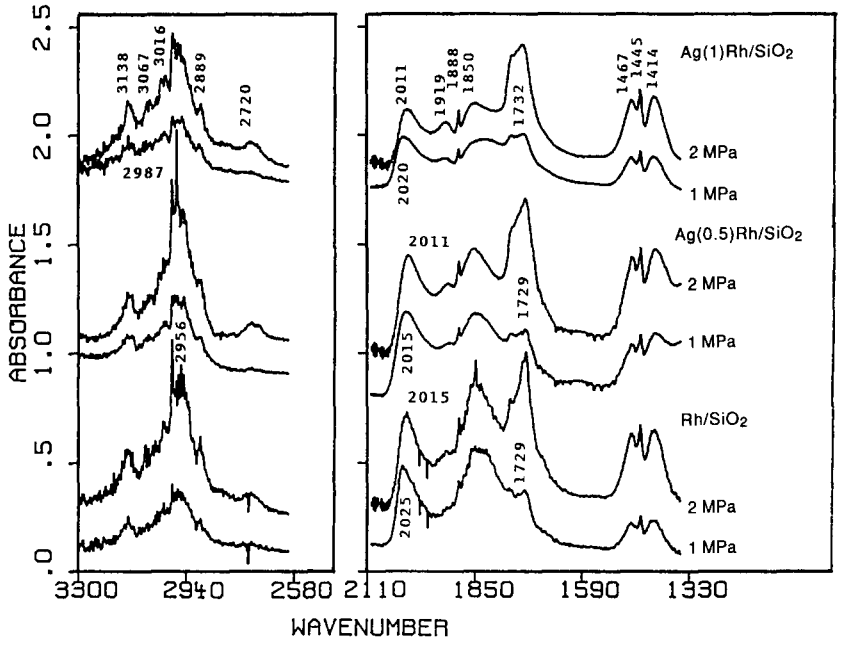

FIG. 5. Infrared spectra of adsorbed species during ethylene hydroformylation at 513 K.

the intensity of bridge CO bands, but slightly decreased the intensity of linear CO bands. An increase in reaction pressure to 2 MPa led to an increase in the formation rate and the selectivity for propionaldehyde, a downward shift of linear and bridge CO wavenumber, and an increase in the intensity of the linear CO, hydrocarbon, and propionaldehyde bands.

DISCUSSION

X-ray diffraction (XRD) studies revealed that Ag and Rh form separate crystallites on SiO_2 support. Average crystallite sizes are 85–136 Å for Rh and 395–468 Å for Ag as shown in Table 1. Large Ag crystallites have been observed on the Ag–Rh/SiO_2 catalysts prepared from Rh and Ag chlorides (*45, 62*). The size of Ag and Rh crystallites depends

TABLE 3

Ethylene Hydroformylation at 513 K

Catalyst	Pressure (MPa)	C_2H_4 conversion		Selectivity			Product ratio
		TOF (sec^{-1})	Rate (mole/kg-hr)	C_2H_6	C_2H_5CHO (mole%)	Other HC	$\frac{C_2H_5CHO}{C_2H6}$
Rh/SiO_2	1	0.17	47.7	77.4	22.2	0.4	0.29
	2	0.18	47.9	71.6	27.3	1.1	0.38
Ag–Rh/SiO_2	1	0.29	50.2	63.1	36.5	0.4	0.58
(0.5 : 1)	2	0.37	64.3	55.1	44.8	0.1	0.81
Ag–Rh/SiO_2	1	1.23	47.7	57.7	42.1	0.2	0.73
(1 : 1)	2	1.29	50.1	49.5	50.4	0.1	1.02

Note. $CO : H_2 : C_2H_4 = 1 : 1 : 1$. Other HC includes CH_4, C_3 + hydrocarbons, and CH_3CHO.

on preparation methods and the type of SiO_2 used (*45, 62*). A fraction of Ag that cannot be observed by XRD pattern appears to deposit on the surface of Rh crystallites. The distribution of Ag on Rh for Ag–Rh/SiO_2 can be inferred from results of XPS and IR studies. A significant decrease in Rh/Si XPS intensity ratio and a marked increase in Ag/Rh XPS intensity ratio with increasing Ag loading indicate Ag species deposits on the Rh surface. The thickness of the Ag layer appears to be great enough to block ejecting of Rh 3*d* electrons.

IR observations of CO and NO adsorption on Ag–Rh/SiO_2 at 301 K can be summarized as the following: (i) the high ratio of linear CO to the bridge CO site indicates that the Rh surface is decorated by Ag species; and (ii) the presence of gem-dicarbonyl bands and the linear CO on Rh^+ as well as a high wavenumber NO^- species suggests that the Rh surface on the Ag(1)Rh/SiO_2 catalyst contains positive charges. The infrared spectra of adsorbed NO is known to be very sensitive to the electronic state of metal and bimetallic surfaces (*59*). The electron-donating or -withdrawing characteristics could lead to either a downward or upward shift of the NO^- band. The upward shift of the NO^- band brought about by Ag indicates that the Rh surface on Ag(1)Rh/SiO_2 is electron-deficient as compared with Rh/SiO_2. XPS results, shown in Fig. 1, also reveal that the oxidation state of Rh on Ag(1)Rh/SiO_2 is between 0 and +1. The presence of Ag appears to promote the formation of isolated Rh^+ sites. Peebles *et al.* (*61*) have found that the transfer of significant net electron density between Ag and Rh takes place at very low Ag coverage on Rh(100) surface. Our results are not sufficient to determine whether such an electron transfer occurs resulting in the formation of Rh^+ on silica supported Ag–Rh catalysts.

Previous studies have shown that a single Rh atom site that chemisorbs linear CO is more active for CO insertion than the Rh ensemble site required for bridge CO; an isolated Rh^+ site is more active for CO insertion than the reduced Rh site (*30*). High C_2 oxygenate activity and selectivity of Ag(1)Rh/SiO_2 might be directly related to the Ag(1)Rh/SiO_2 catalyst containing a high concentration of isolated Rh^+ sites. Nevertheless, linear CO on Rh^+ and gem-dicarbonyl associated with Rh^+ were not observed during reactions. It is unclear whether the Rh^+ site remains on the surface of Ag(1)Rh/SiO_2 under reaction conditions. The absence of linear CO on Rh^+ and gem-dicarbonyl could be due to either their high reactivities or reductive agglomeration of isolated Rh^+ sites (*55*) under reaction conditions.

Both CO hydrogenation and ethylene hydroformylation affect the surface structure of Ag–Rh/SiO_2 catalysts. The IR intensity ratios of the bridge to the linear CO on the Ag–Rh/SiO_2 catalyst under reaction conditions are significantly greater than those under CO adsorption at room temperature. The increased intensity ratio of the bridge to linear CO is likely due to the aggregation of Ag atoms at the expense of interdispersed Ag atoms on the Rh crystallite under reaction conditions. Surface reconstruction induced by adsorbates has been observed for a number of catalytic systems (*63*). Adsorption of CO on small Rh crystallites at 300 K causes the disruption of Rh crystallite and the formation of isolated Rh^+ sites; CO adsorption at temperatures above 423 K leads to reformation of Rh crystallites (*51, 55*).

The difference in the surface structure between characterization and reaction makes it difficult to develop relations between the activity and selectivity of catalysts and the surface characterized before reaction studies. Furthermore, the use of different probe molecules and conditions in catalyst characterization may lead to different conclusions on the surface structure. The high ratio of the linear CO to the bridge CO at 301 K, shown in Fig. 2, suggests that Ag on Rh is highly interdispersed on Ag–Rh/SiO_2. In contrast, the lack of Ag effect on ethane hydrogenolysis on Rh/SiO_2 catalyst at 493 K, shown in Table 1, led to a conclusion

that Ag forms islands on the surface of Rh (*45*). Therefore, caution should be taken in comparing the TOFs shown in Tables 2 and 3 since the number of Rh surface atom used for estimation of the TOF was determined before reaction.

In situ IR observations and simultaneous rate measurements show that the ratio of the bridge CO to the linear CO decreases with increasing Ag content; the rate of formation and selectivity for C_{2+} oxygenates increases with Ag loading during both CO hydrogenation and ethylene hydroformylation. The effect of Ag promotion on C_2 and C_3 oxygenate synthesis can be interpreted in terms of its geometric and electronic effects. The decreased ratio of the bridge to the linear CO sites on Ag–Rh/SiO_2 catalysts should enhance CO insertion selectivity because the single Rh atom site on which the linear CO adsorbs is the active site for CO insertion (*30*). Enhancement of CO insertion selectivity should increase the selectivity for the formation of C_2 oxygenate during CO hydrogenation as well as for the formation of C_3 oxygenate during ethylene hydroformylation.

Methanation has been shown to be structure-insensitive on the Rh single crystal; one metal surface atom site is required for the reaction (*42*). The major effect of Ag on the Rh(111) single crystal is to geometrically block the methanation sites on a one-to-one basis (*42*). The effect of Ag on SiO_2-supported Rh appears to be different from that on the Rh single crystal. If both methanation and CO insertion occurred on the single atom sites, the effect of Ag on the formation of methane and C_2 oxygenates should be similar. Our recent studies of temperature-programmed reaction of CO adsorbed on Ag–Rh/SiO_2 with H_2 shows that the addition of Ag to Rh/SiO_2 shifted the methane peak to higher temperatures; the methane peak temperature shifted progressively from 413 K for Rh/SiO_2 to 615 K for Ag(1)Rh/SiO_2 indicating that Ag additives suppressed methanation activity of Rh catalysts (*64*). The upward shift in methane peak temperature suggests that the electronic effect of Ag may play a role in modifying catalyst activity and selectivity for CO hydrogenation and ethylene hydroformylation.

Although the increase in C_2 and C_3 oxygenate selectivity (i.e., CO insertion selectivity) can be explained by the geometric blockage effect of Ag on the Rh surface, it would be difficult to use simply the geometric effect of Ag to account for the increased rate of formation for C_2 and C_3 oxygenates. Direct evidence for the electronic influence of Ag on Rh/SiO_2 include XPS and IR results at 301 K that show that the presence of Ag on Rh surface promotes a formation of isolated Rh^+ sites. Since Rh^+ is the most active form of surface sites for CO insertion, such a promotion effect of Ag may prevail under reaction conditions resulting in a significant increase in the rate of formation for C_3 oxygenates and in the TOF for ethylene conversion during ethylene hydroformylation. Ag promotion also incenses the rate of formation for C_2 oxygenates; however, it increases the TOF for CO conversion in CO hydrogenation less than it does the TOF for C_2H_4 conversion in C_2H_4 hydroformylation. The less pronounced effect of Ag promotion on CO hydrogenation may be due to the inhibition of methanation brought about by Ag.

Product distributions of CO hydrogenation and ethylene hydroformylation over Rh catalysts depend not only on promoter and support compositions but also on reaction conditions. The effects of reaction temperature on C_2 oxygenate selectivity over Ag–Rh/SiO_2 have been reported in our previous studies (*44*). C_2 oxygenate selectivity increased with temperatures from 473 to 523 K over Rh/SiO_2, Ag(0.25)Rh/SiO_2, and Ag(0.5)Rh/SiO_2; the temperature for maximum C_2 oxygenate selectivity (T_m) occurred at 523 K. In contrast, T_m occurred at 573 K for Ag(1)Rh/SiO_2. Further increasing the temperature above T_m leads to significant increases in rate of formation and selectivity for methane. This is due to the predomi-

nance of CO dissociation and hydrogenation over CO insertion at high temperatures (*7, 8*).

An increase in reaction pressure from 1 to 2 MPa significantly increased the rate of CO insertion as evidenced by the increased rate of formation of C_2 and C_3 oxygenates. Increasing reaction pressure, however, did not result in any obvious variation of *in situ* IR spectra for CO hydrogenation. In contrast, increasing reaction pressures during ethylene hydroformylation decreased the wavenumber of linear CO, but increased its intensity. The decreased wavenumber of adsorbed CO is usually accompanied by decreased intensity due to the decreased dipole–dipole coupling of reduced concentration of adsorbed CO (*56*). One possible explanation for the reverse trend is that high CO pressures increase the surface concentration of adsorbed CO and greatly enhance the formation of adsorbed propionaldehyde which effectively decreases the dipole–dipole coupling between neighboring adsorbed CO.

CONCLUSIONS

The effects of Ag promotion on CO hydrogenation and ethylene hydroformylation over Rh/SiO_2 have been identified as (i) a suppression of methanation and hydrogenation selectivity and (ii) an enhancement of CO insertion activity and selectivity. The combination of these effects results in an increase in the rate of formation and selectivity for C_2 oxygenates during CO hydrogenation and for propionaldehyde (C_3 oxygenate) during ethylene hydroformylation. Catalyst characterization of $Ag–Rh/SiO_2$ by XRD and XPS suggests that part of the Ag forms separate crystallite and part of the Ag deposits on the surface of Rh crystallites. IR study of CO adsorption shows that Ag blocks the bridge CO site on the surface of the Rh crystallite. The ratio of the linear CO to the bridge CO sites increases with Ag loading. A Rh^+ site is observed on $Ag(1)Rh/SiO_2$ by XPS and IR studies of CO and NO adsorption. Exposure of the $Ag–Rh/SiO_2$ catalysts to reactant mixtures under reaction conditions leads to a decrease in the ratio of the linear to the bridge CO sites. The promotion effect of Ag on CO insertion is attributed to a high ratio of the linear CO to bridge CO sites and the possible presence of isolated Rh^+ sites under reaction conditions.

ACKNOWLEDGMENTS

We gratefully acknowledge the partial support of this research by the U.S. Department of Energy (DG-FG-87PC79923) and the Research Challenge Program of the Ohio Board of Regents. We thank Dr. J. Baltrus at PETC for the XPS analysis and Mr. R. Krishnamurthy for assistance in preparation of the tables and typing of the manuscript.

REFERENCES

1. Bhasin, M. M., and O'Connor, G. L., Belgian Patent, 824,822 (1975).
2. Ichikawa, M., *Bull. Chem. Soc. Jpn.* **51,** 2268 (1978).
3. Ichikawa, M., *Bull. Chem. Soc. Jpn.* **51,** 2273 (1978).
4. Bell, A. T., *Catal. Rev. Sci. Eng.* **23,** 203 (1981).
5. Katzer, J. R., Sleight, A. W., Gajardo, P., Michel, J. B., Gleason, E. F., and McMillan, S., *Faraday Discuss. Chem. Soc.* **72,** 121 (1981).
6. Wilson, T. P., Kasai, P. H., and Ellgen, P. C., *J. Catal.* **69,** 193 (1981).
7. Watson, P. R., and Somorjai, G. A., *J. Catal.* **72,** 347 (1981).
8. Watson, P. R., and Somorjai, G. A., *J. Catal.* **74,** 282 (1982).
9. Ichikawa, M., CHEMTECH 674 (1982).
10. Anderson, R. B., "Fischer Tropsch and Related Syntheses." Academic Press, New York, 1983.
11. Sachtler, W. M. H., *in* "Proceedings, 8th International Congress on Catalysis, Berlin, 1984" (G. Ertl, Ed.), Vol. 1, p. 151. Dechema, Frankfurt-am-Main, 1984.
12. Ichikawa, M., Fukushima, T., and Shikakura, K., *in* "Proceedings 8th International Congress on Catalysis, Berlin, 1984" (G. Ertl, Ed.), Vol. 2, p. 69. Dechema, Frankfurt-am-Main, 1984.
13. Orita, H., Naito, S., and Tamaru, K., *J. Catal.* **90,** 183 (1984).
14. Chuang, S. C., Goodwin, J. G., Jr., and Wender, I., *J. Catal.* **92,** 416 (1985).
15. van der berg, F. G. A., Glezer, J. H. E., and Sachtler, W. M. H., *J. Catal.* **93,** 340 (1985).
16. Sachtler, W. M. H., Shriver, D. F., Hollenberg, W. B., and Lang, A. F., *J. Catal.* **92,** 429 (1985).
17. Chuang, S. C., Goodwin, J. G., Jr., and Wender, I., *J. Catal.* **95,** 435 (1985).
18. Chuang, S. C., Tian, Y. H., Goodwin, J. G., Jr., and Wender, I., *J. Catal.* **96,** 396 (1985).

19. Ichikawa, M., and Fukushima, T., *J. Chem. Soc. Chem. Commun.*, 321 (1985).
20. Kawai, M., Uda, M., and Ichikawa, M., *J. Phys. Chem.* **89,** 1654 (1985).
21. van der Lee, G., Schuller, B., Post, T., Favre, T. L. F., and Ponec, V., *J. Catal.* **98,** 522 (1986).
22. van der Lee, G., and Ponec, V., *J. Catal.* **99,** 511 (1986).
23. Sachtler, W. M. H., Shriver, D. F., and Ichikawa, M., *J. Catal.* **99,** 513 (1986).
24. Sachtler, W. M. H., and Ichikawa, M., *J. Phys. Chem.* **90,** 4752 (1986).
25. Gysling, H. J., Monnier, J. R., and Apai, G., *J. Catal.* **103,** 407 (1987).
26. Underwood, R. P., and Bell, A. T., *J. Catal.* **111,** 325 (1988).
27. Yoneda, Y., "Progress in C_1 Chemistry in Japan." Elsevier, Amsterdam/Oxford/New York/Tokyo, 1989.
28. Lavalley, J. C., Saussey, J., Lamotte, J., Breault, R., Hindermann, J. P., and Kiennemann, A., *J. Phys. Chem.* **94,** 5941 (1990).
29. Chuang, S. S. C., Pien, S. I., and Sze, C., *J. Catal.* **126,** 187 (1990).
30. Chuang, S. S. C., and Pien, S. I., *J. Catal.* **135,** 618 (1992).
31. Calderazzo, F., *Angew. Chem. Int. Ed. Engl.* **16,** 299 (1977).
32. Cross, R. J., *in* "Catalysis" (G. C. Bond and G. Webb, Eds.), Vol. 5, p. 366. The Royal Society of Chemistry, London, 1982.
33. Parshall, G. W., "Homogenous Catalysis—The Applications and Chemistry of Catalysis by Soluble Transition Metal Complexes," p. 85. Wiley, New York, 1981.
34. Masters, C., "Homogenous Transition Metal Catalysis—A Gentle Art," p. 102. Chapman & Hall, New York, 1891.
35. Pino, P., Piacenti, F., and Bianchi, M., *in* "Organic Synthesis via Metal Carbonyls" (I. Wender and P. Pino, Eds.), Vol. 2, p. 43. Wiley, New York, 1977.
36. Noack, K., and Calderazzo, F., *J. Organomet. Chem.* **10,** 101 (1967).
37. Chuang, S. S. C., and Pien, S. I., *J. Mol. Catal.* **55,** 12 (1989).
38. Henrici-Olive, G., and Olive, S., "The Chemistry of the Catalyzed Hydrogenation of Carbon Monoxide." Springer-Verlag, New York, 1984.
39. Cotton, F. A., and Wilkinson, G., "Advanced Inorganic Chemistry," p. 1233. Wiley, 1988.
40. Chuang, S. S. C., U.S. Patent, 5,082,977 (1992).
41. Peden, C. H. F., and Goodman, D. W., *Ind. Eng. Chem. Fundam.* **25,** 58 (1986).
42. Goodman, D. W., *in* "Heterogenous Catalysis" (B. L. Shapiro, Ed.), Vol. 2, p. 230. Texas A&M University Press, College Station, 1984.
43. Sinfelt, J. H., "Bimetallic Catalysts: Discoveries, Concepts, and Applications." Wiley, New York, 1983.
44. Chuang, S. S. C., Pien, S. I., and Narayanan, R., *Appl. Catal.* **57,** 241 (1990).
45. Rouco, A. J., and Haller, G. L., *J. Catal.* **72,** 246 (1981).
46. Rouco, A. J., Haller, G. L., Oliver, J. A., and Kemball, C., *J. Catal.* **84,** 279 (1983).
47. Ponec, V., *in* "Advances in Catalysis" (D. D. Eley, H. Pines, and P. B. Weisz, Eds.), Vol. 32, p. 149. Academic Press, New York, 1983.
48. Yang, A. C., and Garland, C. W., *J. Phys. Chem.* **61,** 1504 (1957).
49. Yates, J. T., Jr., Duncan, T. M., Worley, S. D., and Vaughn, R. W., *J. Chem. Phys.* **70,** 1219 (1979).
50. Cavanagh, R. R., and Yates, J. T., Jr., *J. Chem. Phys.* **74,** 4150 (1981).
51. Solymosi, F., Tombacz, I., and Kocsis, M., *J. Catal.* **75,** 78 (1982).
52. Rice, C. A., Worley, S. D., Curtis, C. W., Guin, J. A., and Tarrer, A. R., *J. Chem. Phys.* **74,** 6487 (1981).
53. Worley, S. D., Rice, C. A., Mattson, G. A. Curtis, C. W., Guin, J. A., and Tarrer, A. R., *J. Chem. Phys.* **76,** 20 (1982).
54. Worley, S. D., Rice, C. A., Mattson, G. A., Curtis, C. W., Guin, J. A., and Tarrer, A. R., *J. Phys. Chem.* **86,** 2714 (1982).
55. Solymosi, F., and Pasztor, M., *J. Phys. Chem.* **89,** 4789 (1985).
56. Stoop, F., and Toolenaar, F. J. C. M., and Ponec, V., *J. Catal.* **70,** 50 (1982).
57. van Slooten, R. F., and Nieuwenhuys, B. E., *J. Catal.* **122,** 429 (1990).
58. Solymosi, F., Bansaji, T., and Novak, E., *J. Catal.* **112,** 183 (1988).
59. Arai, H., and Tominga, H., *J. Catal.* **43,** 131 (1976).
60. The Sadtler Standard Spectra, "High Resolution Spectra of Inorganics and Related Compounds." Sadtler Research Laboratories, Inc., Pennsylvania, 1967.
61. Peebles, H. C., Deck, D. D., and White, J. M., *Surf. Sci.* **150,** 120 (1985).
62. Anderson, J. H., Jr., Conn, P. J., and Branderbayer, S. G., *J. Catal.* **16,** 404 (1970).
63. Somorjai, G. A., *Catal. Lett.* **7,** 169 (1990).
64. Krishnamurthy, R., M.S. thesis, The University of Akron, 1992.